Ultrasound in Med. & Biol., Vol. 36, No. 10, pp. 1713–1721, 2010
Copyright © 2010 World Federation for Ultrasound in Medicine & Biology
Printed in the USA. All rights reserved
0301-5629/$ - see front matter

ELSEVIER

doi:10.1016/j.ultrasmedbio.2010.06.014

● *Original Contribution*

ACOUSTIC SIZING OF AN ULTRASOUND CONTRAST AGENT

David Maresca,* Marcia Emmer,* Paul L. M. J. van Neer,* Hendrik J. Vos,* Michel Versluis,† Marie Muller,*‡ Nico de Jong,*†§ and Antonius F. W. van der Steen*§

*Biomedical Engineering Thoraxcentre, Erasmus University Medical Centre, Rotterdam, The Netherlands; †Physics of Fluids Group, University of Twente, Enschede, The Netherlands; ‡Institut Langevin, Université Paris Diderot, ESPCI ParisTech, Paris, France; and §Interuniversity Cardiology Institute of the Netherlands, Utrecht, The Netherlands

(*Received* 11 *January* 2010; *revised* 3 *June* 2010; *in final form* 17 *June* 2010)

Abstract—Because the properties of ultrasound contrast agent populations after administration to patients are largely unknown, methods able to study them noninvasively are required. In this study, we acoustically performed a size distribution measurement of the ultrasound contrast agent Definity®. Single lipid-shelled microbubbles were insonified at 25 MHz, which is considerably higher than their resonance frequency, so that their acoustic responses depended on their geometrical cross sections only. We calculated the size of each microbubble from their measured backscattered pressures. The acoustic size measurements were compared with optical reference size measurements to test their accuracy. Our acoustic sizing method was applied to 88 individual Definity® bubbles to derive a size distribution of this agent. The size distribution obtained acoustically showed a mean diameter (2.5 μm) and a standard deviation (0.9 μm) in agreement within 8% with the optical reference measurement. At 25 MHz, this method can be applied to bubble sizes larger than 1.2 μm in diameter. It was observed that similar sized bubbles can give different responses (up to a factor 1.5), probably because of shell differences. These limitations should be taken into account when implementing the method *in vivo*. This acoustic sizing method has potential for estimating the size distribution of an ultrasound contrast agent noninvasively. (E-mail: d.maresca@erasmusmc.nl) © **2010 World Federation for Ultrasound in Medicine & Biology.**

Key Words: **Acoustic bubble sizing, Ultrasound contrast agent, Definity®, Single bubbles, High frequency, Size distribution.**

INTRODUCTION

Encapsulated gas microbubbles, the constituents of medical ultrasound contrast agents (UCAs), are increasingly used clinically because they showed strong potential for organ perfusion diagnostics, capillary networks imaging and local therapy including drug or gene delivery and sonothrombolysis (Bekeredjian et al. 2005; Dijkmans et al. 2004; Simpson et al. 2001). Commercial UCAs consist of bubble populations ranging from 0.5–10 μm in size and usually exhibit a mean diameter of 1–3 μm.

Ultrasound contrast imaging techniques rely largely on the nonlinear scattering of contrast microbubbles (Eckersley et al. 2005; Simpson et al. 1999). Bubble size has a great impact on the generation of higher harmonic energy scattered by an UCA (Cheung et al. 2005; Goertz et al. 2003). Microbubbles enhance echo contrast the most at their individual resonance frequencies. As an example, Definity® contrast bubbles (Lantheus Medical Imaging, Inc., North Billerica, MA, USA) are estimated to have a resonance frequency of 75 MHz for a bubble diameter of 0.5 μm, 27 MHz for a diameter of 1 μm and 10 MHz for a diameter of 2 μm (Goertz et al. 2007). Thus, ultrasound contrast imaging techniques benefit from different sized groups of an agent population depending on the frequency of the ultrasound field applied (Goertz et al. 2006a). Contrast echocardiography or contrast liver imaging work in the 1–7 MHz range (Feinstein 2004; Hohmann et al. 2003), whereas contrast intravascular ultrasound (Goertz et al. 2006b) works in the 20–40 MHz range. Therefore, it is important to know the size distribution of an UCA.

Standard particle size analyzers used to measure an UCA size distribution *in vitro* can be based on to the change of electric conductance of particles in a solution (Coulter principle), on laser diffraction of these particles (*e.g.*, Mastersizer 2000, Malvern Instruments Ltd., Worcestershire, UK) or on the optical scanning of an

Address correspondence to: David Maresca, Biomedical Engineering, Erasmus Medical Centre, Room Ee2218, Dr. Molenwaterplein 50, 3015 Rotterdam, The Netherlands. E-mail: d.maresca@erasmusmc.nl

agent population using a microscope (Alter et al. 2009). However, the size distribution of UCA populations after human administration is unknown. Factors such as the gas concentration of the bubbles inside the body, the temperature elevation to 37°C (Vos et al. 2008) and the lung filtering of the largest bubbles (Bouakaz and de Jong 2007; Lindner et al. 2002) make comparison with *in vitro* size distribution measurements unreliable. It is therefore of interest to offer experimental methods to measure UCA size distributions noninvasively (Adam et al. 2005).

Newhouse and Mohana Shankar (1984) presented an ultrasound-based double-frequency method of sizing bubbles, already envisioning the study of contrast agents for echocardiography as a potential application. Gas bubbles respond to a dual-frequency excitation by returning a signal at plus and minus the two frequencies, at resonance only. From the knowledge of the resonance frequency of a gas bubble, the radius can be readily determined. This idea was developed further (Cathignol et al. 1990) and an instrument to size and analyze bubbles with this technique was built and tested (Magari et al. 1997). However, this double-frequency technique needs at least two transducers and was applied to size bubbles bigger than 30 μm only. Leighton et al. (1996) suggested to size bubbles using ultrasound by applying eight different ultrasound methods simultaneously (*e.g.*, broadband scattering, fundamental or harmonic scattering, two frequencies mixing at resonance). The limitations and advantages of the different methods compensate each other, providing a sharper size estimation. The approach was successfully applied to a single gas bubble of radius 0.9 mm. None of these studies used high-frequency ultrasound (>10 MHz).

Unfortunately, the resonance frequency of an encapsulated bubble is not an unambiguous determinant of its size because of the shell influence. Other research groups developed methods to determine the size distribution of lipid-shelled bubble clouds *in vitro* by fitting attenuation or backscattering simulations to their experimental acoustic pulse attenuation or scattering measurements (Coussios et al. 2004; Rossi et al. 2010). In this study, we suggest inspecting bubbles high above their resonance frequencies. In this condition, bubble responses depend on their geometrical cross section only, quasi-independent from their shell elasticity and viscosity (Sijl et al. 2008). Our objective was to take advantage of this feature to measure single bubble radii using ultrasound in pulse-echo mode. Such a noninvasive method can potentially be exploited to estimate the size distribution of an UCA *in vivo*.

An acoustic sizing method was developed in our laboratory and applied to a population of 88 individual Definity® bubbles. The result is compared with an optical size measurement of the same bubbles. The theoretical background of this method is introduced and particular attention is given to the measurement system and its calibration, which enabled the derivation of the size of an UCA bubble from its echo amplitude.

Theoretical background

In this section, we are going to derive the equation to determine a bubble radius out of the acoustic pressure impinging on that bubble, the acoustic pressure scattered back by the bubble and the bubble-transducer distance.

A gas bubble of radius R, insonified by an ultrasound wave of wavelength λ, scatters an omnidirectional pressure wave if $R \ll \lambda$ is assumed.

The power scattered by the bubble, P_s, relates to the incident wave intensity, I_i, as $P_s = \sigma I_i$, where σ is the acoustic scattering cross section (Medwin 1977).

The intensity scattered by a point source is equal to the quotient of the scattered power and the spherical surface at distance z. For a spherical gas bubble, the incident and scattered intensities relate as:

$$I_s = \frac{\sigma I_i}{4\pi z^2}, \tag{1}$$

where I_s is the scattered intensity.

For harmonic plane waves, the intensity can be formulated as the quotient of the acoustic pressure squared divided by twice the acoustic impedance. Thus equation (1) can be rewritten as:

$$p_s = \frac{1}{z}\sqrt{\frac{\sigma}{4\pi}}p_i, \tag{2}$$

where p_i is the incident pressure that hits the bubble and p_s the pressure scattered by the bubble.

Medwin (1977) has shown that the acoustic scattering cross section of a gas bubble in a liquid environment is expressed in the linear regime as:

$$\sigma(R,f) = \frac{4\pi R^2}{\left\{\left(\frac{f_0(R)^2}{f^2}\right)-1\right\}^2 + \delta(R,f)^2}, \tag{3}$$

where f is the frequency of the applied ultrasound field, f_0 the resonance frequency of the bubble and δ the total damping. This equation is also valid for encapsulated bubbles in the linear regime.

The damping δ^2 for the microbubbles in this study is assumed to be much smaller than 1 (Goertz et al. 2007; Leighton 1994). It follows that for $f >> f_o$, the acoustic scattering cross section becomes a function of R only:

$$\sigma(R,f) = 4\pi R^2, \tag{4}$$

Combining eqns (2) and (4) at the bubble wall leads to:

$$p_s(R) = p_i(R), \tag{5}$$

The scattered pressure is equal to the incident pressure at the bubble wall. As $R \ll \lambda$, the pressure distribution over the bubble wall is homogeneous and the pressure wave is scattered equally in every direction.

The pressure scattered at a distance z can be calculated using energy conservation in a lossless medium:

$$p_s^2(z) = \frac{4\pi R^2}{4\pi z^2} p_s^2(R), \tag{6}$$

Combining eqns (5) and (6), the bubble radius is expressed as:

$$R = z\frac{p_s(z)}{p_i(R)}, \tag{7}$$

Equation (6) states that, for $f >> f_o$, the radius of a bubble can be derived from its backscattered pressure once the distance and the pressure impinging on the bubble wall are known. This holds for lipid-shelled bubbles as well as gas bubbles.

METHODS

Measurement system overview

The combined optical and acoustic single-bubble size measurement setup (Fig. 1) consisted of an arbitrary waveform generator (AWG520, Tektronix, Beaverton, OR, USA) and a 60-dB RF linear power amplifier (LPI-10, ENI, Rochester, NY, USA) linked to generate and amplify the transmit pulses (25MHz, 30% bandwidth Gaussian pulses). A low-noise amplifier (Miteq, Hauppauge, NY, USA) amplified the received signals by 60 dB. These were then digitized at 200 MHz by a 12-bit A/D PCI-card (DP310, Acqiris, Geneva, Switzerland). A 25-MHz single-element focused transducer (Panametrics NDT, 1-inch focus, 54% −6 dB bandwidth; Olympus NDT, Waltham, MA, USA) was mounted to a water tank. The UCA Definity® was injected with a syringe in a 200-μm diameter cellulose capillary (Spectrum Laboratories Inc., 132294, Breda, The Netherlands), which crossed the transducer beam focus inside the water tank. The tank holding the transducer and the capillary was placed on the translation stage of a microscope (Olympus BH-2 research microscope, Olympus Corporation, Zoeterwoude, The Netherlands) equipped with a water immersion objective lens (Olympus LUMPLFLN 40XW, N.A. 0.8) focused on the capillary tube. A charge-coupled device (CCD) camera (Lm165M, Lumenera Corporation, Ottawa, ON, Canada) was mounted on the microscope and used to record images of the capillary region of interest, where both the microscope and the acoustic beam were in focus. An optical fiber was fixed below the water tank to illuminate the microscope focal plane with a continuous light source.

Transducer calibration

To measure the incident pressure received by a bubble at the transducer focus, as well as the pressure backscattered by the same bubble on the transducer surface, the transducer was carefully calibrated both in emission and in reception. This complete characterization was performed at 25 MHz based on two independent measurements. First, a calibrated hydrophone setup (75-μm polyvinylidene fluoride needle hydrophone, Precision Acoustics Ltd., Dorchester, Dorset, UK) was used to measure the pressure at focus and to determine the transmit transfer function of the transducer (van Neer et al. 2007). For our experimental conditions, we measured a pressure at focus of 390 kPa and a transmit transfer function of 3.2 kPa/V. The uncertainty of the hydrophone at 25 MHz was ±12%. Note that the calculation of this transmit transfer function was done using a transducer gain corrected for water attenuation. Our transducer had a focal distance of 2.6 cm that resulted in an attenuation in water of 3.3 dB at 25 MHz. Second, a pulse-echo setup, using a flat aluminum reflector at the

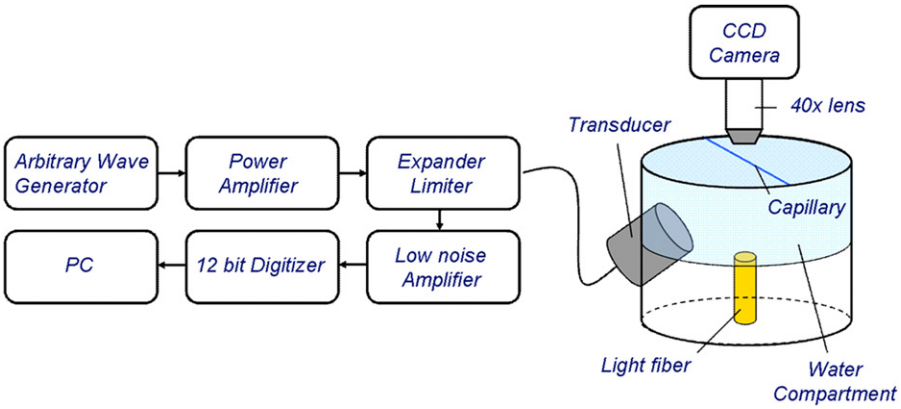

Fig. 1. Schematic overview of the experimental setup for optical and acoustical sizing of microbubbles, using an acoustically and optically transparent capillary tube.

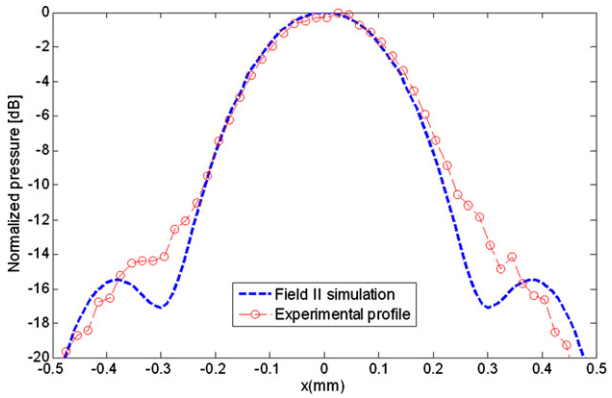

Fig. 2. Comparison of the experimental lateral beam profile at focus of the 25-MHz transducer (*dotted circled curve*) with its simulated profile (*dotted curve*).

transducer focus, enabled the measurement of the product of the transmit transfer function and the receive transfer function of the transducer (van Neer et al. 2007). By combining the results of these two measurements, we derived the receive transfer function, which was 26.0 μV/Pa. The knowledge of the receive transfer function, R_t, at 25 MHz made the conversion of the digitized backscattered bubble echoes into pressure values possible.

To determine the pressure variation near the focal spot of the transducer beam, we performed a lateral beam profile at focus. The measurement was compared with a Field II simulation (Jensen and Svendsen 1992). Figure 2 shows both the simulation and the experiment. The pressure drops by 1 dB 80 μm away from the absolute focus.

Because the hydrophone chosen for this study exhibits a diameter in the order of a wavelength at 25 MHz, we calculated the spatial averaging that will affect the incident pressure field estimates. Following the theory detailed by Radulescu et al. (2001), together with our Field II–simulated pressure values, we obtained a pressure drop at focus of 0.12 dB because of spatial averaging. Thus, we concluded that spatial averaging has a negligible impact on our study.

Circuit characterization in reception

The transducer receive transfer function, R_t, was defined (van Neer et al. 2007) as:

$$R_t = \frac{V_{Open}^{Tx}}{p_s}, \tag{8}$$

where V_{open}^{Tx} is the open circuit voltage produced by the transducer and p_s the pressure backscattered by a bubble on the transducer surface.

To obtain V_{open}^{Tx}, the received amplitudes have to be converted from digitizer voltages to open circuit voltages. The receive chain of the circuit consisted of the transducer connected to the expander/limiter, the low-noise amplifier, a band-pass filter (3 to 35 MHz, fifth-order Butterworth) and the digitizer. The reception circuit is represented in Fig. 3.

We can link the backscattered pressure, p_s, to the digitizer voltage, V_d, by:

$$p_s = \frac{1}{R_t}\left(\frac{Z_T + Z_C}{Z_C}\right)\frac{V_d}{T_{V_d \to V_c}}, \tag{9}$$

where Z_T is transducer electric impedance, Z_c the receive circuit impedance, V_c the received signal voltage before amplification and $T_{Vd \to Vc}$ the transfer ratio accounting for amplification, the filter and the coaxial cables.

We measured with a vector impedance meter (4193A, Hewlett Packard, Yokogawa, Japan) Z_T and Z_c and found 46.9 Ohms and 40.7 Ohms, respectively. $T_{Vd \to Vc}$ was measured by linking the reception circuit to the AWG520 and simulating a received pulse of 1.1 mV amplitude. We found a corresponding voltage of 200 mV. We derived from these measures that $T_{Vd \to Vc}$, which is equal to the ratio of V_d over V_c, and obtained a value of 182.

The knowledge of Z_T, Z_c, $T_{Vd \to Vc}$ and R_t fully characterized the circuit in reception and allowed the exact

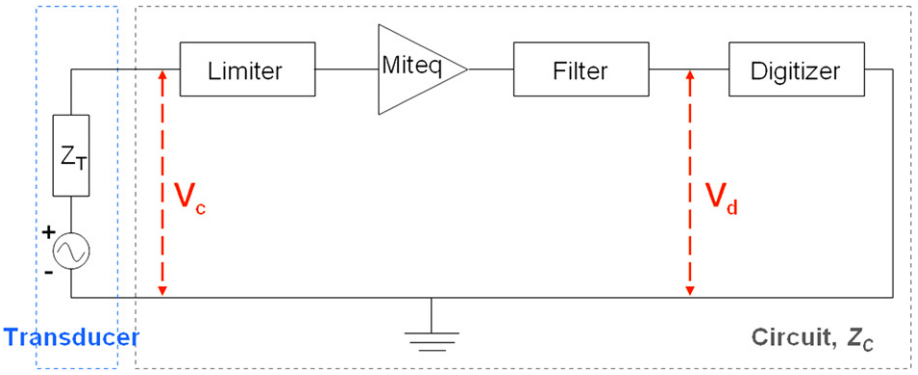

Fig. 3. Schematic overview of the receive circuit. V_d is the voltage at the digitizer leads and V_c the voltage at the input. Z_T is transducer impedance and Z_C the receive circuit impedance.

conversion of the digitized bubble echoes from voltage amplitudes into real pressures.

Optical and acoustic size measurements

A low concentration of Definity® microbubbles was injected into the capillary using a syringe, to have no more than one bubble per capillary section of 200 μm. The flow in the capillary was controlled using a manual syringe pump. Thanks to that flow control, single bubbles were kept one by one in the capillary region of interest, where both the transducer beam and the microscope are focused.

For each single bubble studied, 64 RF signals were recorded. Simultaneously, an image of the corresponding bubble was captured with the CCD camera. The size of the bubble of interest was determined from the microscope image using a minimum-cost algorithm that delimits the contour of the bubble by finding the steepest grayscale gradient in a box set around the bubble (Fig. 4). The optical observation of the diameters before and after insonification revealed no alteration of the bubble sizes. The systematic error on the optical size measurement of a bubble was estimated by using a calibrated grid displaying dot patterns (DA020, Max Levy Autograph, Philadelphia, PA, USA). The algorithm was used to measure the size of 20 calibrated dots from the grid, and the variation of the results was investigated. The random error was estimated by sizing the same bubble on different images. Combining the random and the systematic error, we quantified the uncertainty of the optical size measurement to be 0.2 μm.

The acoustic sizing was based on the accurate knowledge of the distance between the bubble of interest and the transducer, the pressure at the transducer focus (390kPa) and the pressure backscattered by that bubble on the transducer surface. The bubble-transducer distance was derived from the time of flight of the digitized bubble echoes. The backscattered pressures were determined as follows. For each bubble studied, 64 RF signals were acquired. Because the capillary flow could not be completely stopped, the bubbles of interest were moved back and forth around the highest echo position using the manual syringe pump. This movement had a typical amplitude of 50 μm. Among the 64 signals acquired per bubble, one had the highest amplitude. That signal was chosen because it corresponds to the closest position of a given bubble from the exact transducer beam focal point. These selected backscattered amplitudes were converted into a pressure value knowing the receive transfer of the transducer. We evaluated the uncertainty of the acoustic size measurement to be 24% of the estimated bubble diameter, which corresponds to an error of 0.7 μm for a bubble of 3 μm. It originates from the 12% uncertainty of the incident and scattered pressure values. The uncertainty of the bubble−transducer distance was negligible.

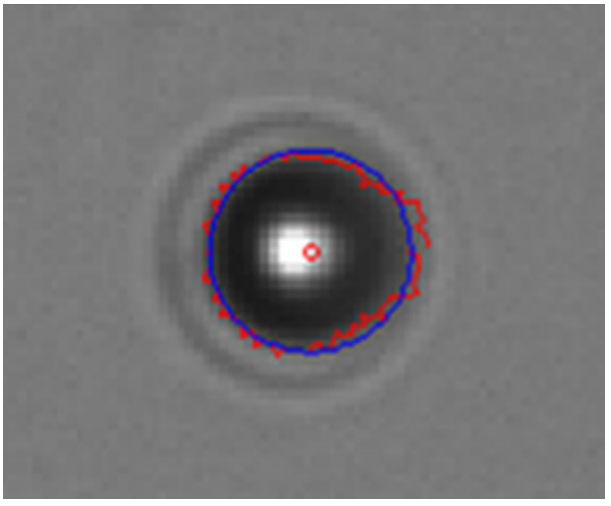

Fig. 4. Contour detection of a contrast bubble for optical sizing. The red curve corresponds to the steepest color gradient detection and the blue contour is the best circular fit from the red contour.

RESULTS

Experimental and simulated backscattered pressures

A set of 88 Definity® microbubbles was characterized both optically and acoustically. The experimental backscattered pressure values were plotted as a function of the optical reference diameters and compared with theory (Fig. 5). We calculated the time responses of individual bubbles using the nonlinear Marmottant model (Marmottant et al. 2005) and derived the theoretical

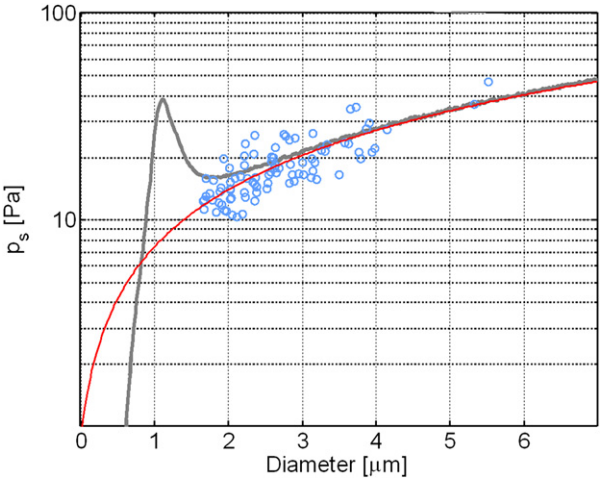

Fig. 5. Comparison of the theoretical and experimental backscattering of individual Definity® microbubbles as a function of their diameters. The blue circles represent the 88 experimental data points, the red curve is the linear fit of the experimental data and the gray curve is the behavior predicted by the nonlinear Marmottant model.

backscattered pressure values from these time responses. The input for the simulation were Definity® shell parameters determined in our frequency range (Goertz et al. 2007) combined with our experimental settings (25 MHz, 390 kPa at transducer focus, transducer-to-bubble distance of 2.6 cm). The experimental data points showed the linear trend expected above resonance from the simulation. Note that for a given bubble diameter, the amplitude of the scattering varied up to a factor 1.5, which is in agreement with previous findings (Emmer et al. 2009).

Size distributions

The size distribution obtained with our acoustic method resulted in a mean diameter of 2.45 μm and a standard deviation of 0.85 μm. As a comparison, the optical characterization of the same 88 microbubbles featured a mean diameter of 2.67 μm and a standard deviation of 0.78 μm. In terms of medians, the acoustic distribution exhibits a value of 2.22 μm and the optical one a value of 2.55 μm (Table 1). The maximum diameter measured acoustically was 6.2 μm and corresponds to an optical diameter of 5.5 μm. The minimum acoustic diameter measured was 1.4 μm and the optical one measured 1.7 μm. As a comparison, Lantheus Medical Imaging claims for Definity® a mean diameter range of 1.1−3.3 μm and a percentage of bubbles showing a diameter inferior to 10 μm of 98%.

The acoustic diameters and the optical ones are compared in Fig. 6, showing a correlation coefficient of 0.9. The optical and acoustic size distributions are represented in Fig. 7. The diameter range of the optical distribution was divided into 20 columns, resulting in a bin size of 0.20 μm. The same bin size was used for the acoustic size distribution.

DISCUSSION

The individual microbubble diameters measured acoustically show a very good agreement with the diameters measured optically, which validates our acoustic sizing method. The experimental data follows the expected linear scattering trend above resonance. The agreement with the Marmottant model, using Definity® shell parameters in the frequency range 12−28 MHz, is excellent. This work also exhibits an unexpected spread of the data points that is not predicted by the current model. We observed a maximum deviation of a factor 1.5 relative to the model. For the smallest bubbles measured, which have a resonance frequency close to 25 MHz (Goertz et al. 2007), the data confirms that lipid-shelled gas bubbles of equal size show scattering variations in amplitude (Emmer et al. 2009). Our sizing

Table 1. Comparison of the optical and acoustic size measurement of 88 Definity® microbubbles

88 Definity bubbles study	Optical reference characterization	Acoustic characterization	Variation between measurements
Mean diameter (μm)	2.67	2.45	8%
Median diameter (μm)	2.55	2.22	13%
Standard deviation (μm)	0.78	0.85	8%

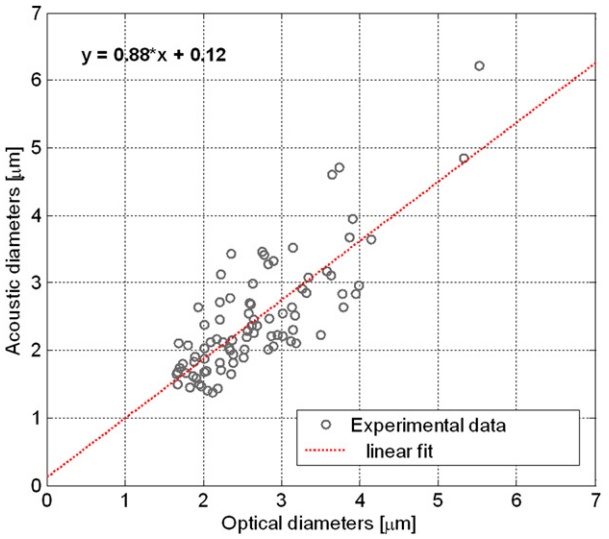

Fig. 6. Correlation between the acoustic and the optical diameters determined experimentally.

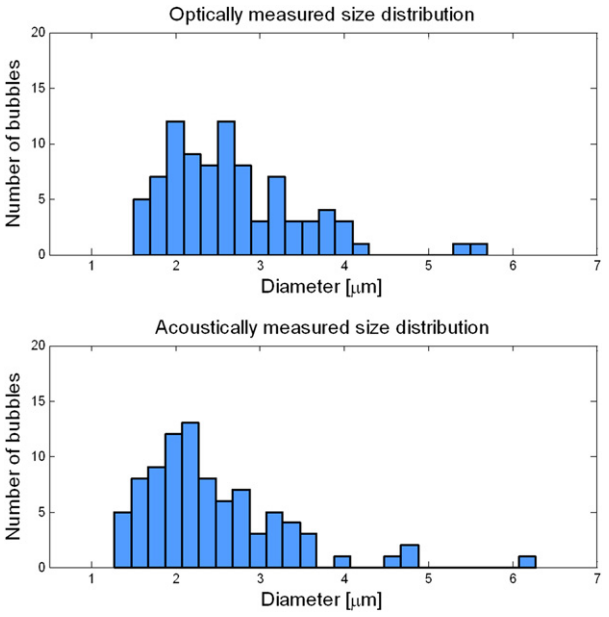

Fig. 7. Optical (*top*) and acoustic (*bottom*) size distributions of the same population of 88 Definity® bubbles.

approach would benefit from the development of lipid-shelled bubbles that have equal scattering properties at a given size, contrary to the bubbles used in this study. Moreover, the choice of the ultrasound frequency of investigation will determine the smallest bubbles that can be sized accurately, because bubbles smaller than a certain size will violate the linear scatterer assumption. For Definity® and at 25 MHz, we can establish sizes greater than 1.2 μm diameter (Goertz et al. 2007). By increasing the ultrasound frequency of investigation, smaller bubble sizes can be measured.

The acoustically determined size distribution is comparable in shape with the optical one. The acoustic size distribution appears slightly wider in terms of diameter range and shifted towards the lower radii by 8%. The $\pm$12% uncertainty of the hydrophone used to calibrate the transducer is thought be one of the reasons for the observed global shift, because the calibration of the transducer sensitivity in reception governs the bubble size estimation. The total damping, which was neglected in this study, can also have a small impact on the distribution because its contribution increases with bubble size. For Definity® bubble diameters of 1.3 μm and 6 μm, which are the boundaries of our size measurement range, the total damping squared was estimated, respectively, to be 0.02 and 0.1 using the equations used by Goertz et al. (2007). Local disparities between the two distributions partly originate from the scattering variations of lipid-shelled microbubbles for a given size. If a bubble is not scattering at its full potential, it will "sound" like a smaller one.

Other factors may explain the remaining differences between these two measurements. First, a tube made of cellulose was used because this material absorbs a large amount of water and is expected to have an acoustic impedance matching reasonably well with water. However, the capillary influence on the pressure value measured with the hydrophone at the transducer focus is not accurately known. Each ultrasound pulse travels twice through the cellulose wall of the capillary (transmission and reception), which may cause an attenuation of the ultrasound waves and which would tend to globally shift the acoustic distribution toward lower radii. Second, the pressure amplitude along the cross section of the capillary tube is not distributed homogeneously. To verify that experimentally, we inserted a 30-μm tungsten wire in a 200-μm cellulose capillary and compared the amplitude of the echo backscattered by the system wire plus capillary with the echo amplitude of the tungsten wire alone. We measured an increase in amplitude of a factor 1.9, with 20-MHz Gaussian pulses of 50% bandwidth for the system wire plus capillary. Others such as Qin et al. (2008) simulated for different tube materials that the peak pressure within the tube can rise up to 300% of the incident pressure amplitude. As a consequence, the bubbles might have been excited at higher or lower pressures than 390 kPa, depending on their exact position in the tube during data acquisition.

Another parameter difficult to control was the position of the bubble under consideration along the tube axis. Each candidate was kept in the transducer focal region but the position of the bubble was not stable during the acoustic data acquisition. If the bubble of interest was not located at the focal point where the pressure was measured with the hydrophone, it received an incident pressure slightly lower than the pressure expected at focus. Experimentally, the beam profile of the transducer tells us that at a lateral distance of 80 μm from the focus, the pressure amplitude drops by 1 dB only. We solved this problem by selecting the highest echo amplitude out of the 64 acquired per bubble, because the maximal scattering will occur at the transducer focal point. Experimentally, the bubble of interest was kept in the ultrasound beam focal region using a manual syringe pump and going back and forth around the maximum scattering position.

The acoustic bubble sizing method presented in this study proved to be competitive in determining the size distribution of an UCA. It benefits from the usual advantages of ultrasound imaging techniques, *e.g.*, potentially real-time, noninvasive, harmless for the patient and affordable. Despite the current work focused on studying a lipid-shelled ultrasound contrast agent, the technique could be applied to any type of gas bubbles, independent of the nature of their shell because only the geometric scattering of these microspheres is important. This method could be the core principle running an "acoustic Coulter counter" instrument and used to test UCA filtrations before administration to patients. The next step envisioned is to analyze UCA populations in superficial arteries (*e.g.*, carotid artery) because the method is noninvasive. Such an examination would give extra information on the change in the size parameters that an UCA population experiences after patient administration and it would help designing microbubble size distributions dedicated to a given clinical application. However, to apply our sizing approach *in vivo*, some challenges will have to be overcome. Working at high frequencies limits the penetration depth because of tissue and blood attenuation. As a consequence, some bubbles may see their signals lost in the system noise. It is possible to use clinical scanners to image single bubbles as shown by Klibanov et al. (2002). This was achieved at lower frequencies, emitting at 1 MHz and receiving at 3 MHz. On the basis of our experimental results—pressure values of single Definity® bubbles are $>$10 Pa—we believe that high-end scanners (signal-to-noise ratio $<$1 Pa) working at our frequency range should also be able to detect single

bubbles. A single bubble flowing in the carotid artery (2.5 cm deep, 0.5 dB/cm/MHz attenuation) should give a response above the noise level if the incident pressure is increased to the MPa range (*e.g.*, 4MPa) to compensate for attenuation. An absolute size distribution measurement *in vivo* would require the exact knowledge of the tissue attenuation. However, even without that knowledge, a relative measurement of the standard deviation of a bubble population could be performed. Another issue is the calibration of the ultrasound beam and the possible presence of resonant bubbles depending on the frequency of the imaging modality (*e.g.*, 15 MHz for 3-D carotid imaging). Moreover, the success of this technique depends on single bubbles passing through the focus one by one; otherwise, their size might be significantly underestimated. A solution would be to use two frequencies of the same transducer. To determine a bubble position with respect to the acoustic axis, two consecutive pulses of 20 and 30 MHz can be transmitted, taking advantage of the beam profile differences at both frequencies. A bubble is considered on axis when the difference in backscattered amplitudes at the two frequencies is minimal. The knowledge of the bubble positions, required to estimate their size acoustically, could be determined using a 3-D probe. Although temperature elevation to 37°C and viscosity change in the bloodstream may affect the shell properties of UCAs, the acoustic sizing method presented here should still provide meaningful statistical results because it relies on the microspheres' geometry.

Acknowledgment—Funding for this work was provided by the Simon Stevin grant 2007 of the Dutch Technology Foundation (STW). The agent Definity® was provided by Lantheus Medical Imaging. We thank Geert Springeling and Robert Beurskens for their contribution to the experimental setup, Klazina Kooiman for her suggestions on microbubble handling, Frits Mastik for discussion and support with contour detection of bubbles for optical sizing and Mike Danilouchkine for his guidance with lateral beam profile measurements.

REFERENCES

Adam D, Sapunar M, Burla E. On the relationship between encapsulated ultrasound contrast agent and pressure. Ultrasound Med Biol 2005; 31:673−686.

Alter J, Sennoga CA, Lopes DM, Eckersley RJ, Wells DJ. Microbubble stability is a major determinant of the efficiency of ultrasound and microbubble mediated in vivo gene transfer. Ultrasound Med Biol 2009;35:976−984.

Bekeredjian R, Grayburn PA, Shohet RV. Use of ultrasound contrast agents for gene or drug delivery in cardiovascular medicine. J Am Coll Cardiol 2005;45:329−335.

Bouakaz A, de Jong N. WFUMB safety symposium on echo-contrast agents: Nature and types of ultrasound contrast agents. Ultrasound Med Biol 2007;33:187−196.

Cathignol D, Chapelon JY, Newhouse VL, Shankar PM. Bubble sizing with high spatial-resolution. IEEE Trans Ultrason Ferroelectr Freq Control 1990;37:30−37.

Cheung K, Couture O, Bevan PD, Burns PN, Foster FS. The effect of bubble size distribution and driving frequency on the "subharmonic" response from Definity microbubbles. IEEE Ultrason Symp 2005; 850−853.

Coussios CC, Holland CK, Jakubowska L, Huang SL, MacDonald RC, Nagaraj A, McPherson DD. In vitro characterization of liposomes and Optison (R) by acoustic scattering at 3.5 MHz. Ultrasound Med Biol 2004;30:181−190.

Dijkmans PA, Juffermans LJ, Musters RJ, van Wamel A, ten Cate FJ, van Gilst W, Visser CA, de Jong N, Kamp O. Microbubbles and ultrasound: From diagnosis to therapy. Eur J Echocardiogr 2004;5: 245−256.

Eckersley RJ, Chin CT, Burns PN. Optimising phase and amplitude modulation schemes for imaging microbubble contrast agents at low acoustic power. Ultrasound Med Biol 2005;31:213−219.

Emmer M, Vos HJ, Versluis M, de Jong N. Radial Modulation of Single Microbubbles. IEEE Trans Ultrason Ferroelectr Freq Control 2009; 56:2370−2379.

Feinstein S. The powerful microbubble: From bench to bedside, from intravascular indicator to therapeutic delivery system, and beyond. Am J Physiol Heart Circ Physiol 2004;287:450−457.

Goertz DE, Frijlink M, Bouakaz A, Chin CT, de Jong N, van der Steen AF. The effect of bubble size on nonlinear scattering from microbubbles at high frequencies. IEEE Ultrason Symp 2003; 1503−1506.

Goertz DE, Frijlink ME, de Jong N, van der Steen AFW. High frequency nonlinear scattering from a micrometer to submicrometer sized lipid encapsulated contrast agent. Ultrasound Med Biol 2006a;32: 569−577.

Goertz DE, Frijlink ME, Tempel D, van Damme LC, Krams R, Schaar JA, Ten Cate FJ, Serruys PW, de Jong N, van der Steen AF. Contrast harmonic intravascular ultrasound: A feasibility study for vasa vasorum imaging. Invest Radiol 2006b;41: 631−638.

Goertz DE, de Jong N, van der Steen AF. Attenuation and size distribution measurements of Definity(Tm) and manipulated Definity(Tm) populations. Ultrasound Med Biol 2007;33:1376−1388.

Hohmann J, Albrecht T, Hoffmann CW, Wolf KJ. Ultrasonographic detection of focal liver lesions: Increased sensitivity and specificity with microbubble contrast agents. Eur J Radiol 2003;46: 147−159.

Jensen JA, Svendsen NB. Calculation of pressure fields from arbitrarily shaped, apodized, and excited ultrasound transducers. IEEE Trans Ultrason Ferroelectr Freq Control 1992;39:262−267.

Klibanov AL, Rasche PT, Hughes MS, Wojdyla JK, Galen KP, Wible JH, Brandenburger GH. Detection of individual microbubbles of an ultrasound contrast agent: Fundamental and pulse inversion imaging. Acad Radiol 2002;9:S279−S281.

Leighton TG. The acoustic bubble. London: Academic Press Limited; 1994.

Leighton TG, Phelps AD, Ramble DG, Sharpe DA. Comparison of the abilities of eight acoustic techniques to detect and size a single bubble. Ultrasonics 1996;34:661−667.

Lindner JR, Song J, Jayaweera AR, Sklenar J, Kaul S. Microvascular rheology of Definity microbubbles after intra-arterial and intravenous administration. J Am Soc Echocardiogr 2002;15: 396−403.

Magari PJ, Kline-Schoder RJ, Stoedefalke BH, Butler BD. A noninvasive, in-vivo, bubble sizing instrument. IEEE Ultrason Symp 1997;1205−1210.

Marmottant P, van der Meer S, Emmer M, Versluis M, de Jong N, Hilgenfeldt S, Lohse D. A model for large amplitude oscillations of coated bubbles accounting for buckling and rupture. J Acoust Soc Am 2005;118:3499−3505.

Medwin H. Counting bubbles acoustically: a review. Ultrasonics 1977; 15:7−13.

Newhouse VL, Mohana Shankar P. Bubble size measurements using the nonlinear mixing of two frequencies. J Acoust Soc Am 1984;75: 1473−1477.

Qin SP, Kruse DE, Ferrara KW. Transmitted ultrasound pressure variation in micro blood vessel phantoms. Ultrasound Med Biol 2008;34: 1014−1020.

Radulescu EG, Lewin PA, Goldstein A, Nowicki A. Hydrophone spatial averaging corrections from 1 to 40 MHz. IEEE Trans Ultrason Ferroelectr Freq Control 2001;48:1575−1580.

Rossi S, Waton G, Krafft MP. Phospholipid-coated gas bubble engineering: Key parameters for size and stability control, as determined by an acoustical method. Langmuir 2010;26:1649−1655.

Sijl J, Gaud E, Frinking PJ, Arditi M, de Jong N, Lohse D, Versluis M. Acoustic characterization of single ultrasound contrast agent microbubbles. J Acoust Soc Am 2008;124:4091−4097.

Simpson DH, Chin CT, Burns PN. Pulse inversion Doppler: A new method for detecting nonlinear echoes from microbubble contrast agents. IEEE Trans Ultrason Ferroelectr Freq Control 1999;46: 372−382.

Simpson DH, Burns PN, Averkiou MA. Techniques for perfusion imaging with microbubble contrast agents. IEEE Trans Ultrason Ferroelectr Freq Control 2001;48:1483−1494.

van Neer P, Matte G, Sijl J, Borsboom JMG, de Jong N. Transfer functions of US transducers for harmonic imaging and bubble responses. Ultrasonics 2007;46:336−340.

Vos HJ, Emmer M, de Jong N. Oscillation of single microbubbles at room versus body temperature. IEEE Ultrason Symp 2008; 982−984.